Scientia Iranica B (2011) 18 (4), 974–985

SCIENTIA IRANICA

Sharif University of Technology

Scientia Iranica

Transactions B: Mechanical Engineering

www.sciencedirect.com

Buoyancy-assisted flow reversal and combined mixed convection–radiation heat transfer in symmetrically heated vertical parallel plates: Influence of two radiative parameters

F. Bazdidi-Tehrani *, **H. Nazaripoor**

School of Mechanical Engineering, Iran University of Science and Technology, Tehran, P.O. Box 16846-13114, Iran

Received 24 January 2011; revised 30 April 2011; accepted 23 May 2011

KEYWORDS

Mixed convection;
Radiative heat transfer;
Vertical parallel plates;
Finite volume method;
Discrete ordinates method;
Flow reversal;
Fanning friction coefficient.

Abstract The present article encompasses the laminar ascending flow and combined mixed (free and forced) convective-radiative heat transfer within symmetrically heated vertical parallel plates. Radiative heat transfer between two opposite walls is considered and the gas is assumed as gray, absorbing, emitting and scattering. Elliptic governing equations for the case of buoyancy assisted flow are solved numerically employing a home-made CFD code based on the finite volume method. The radiative transfer equation is solved using the discrete ordinates method, adopting its S_6 quadrature scheme. The influence of two important radiative parameters, namely, wall emissivity and scattering albedo, while the extinction coefficient is either constant or not, on the occurrence of flow reversal, fanning friction coefficient, flow and thermal fields, is investigated. Present results show that the occurrence of reversed flow enhances both heat transfer and the fanning friction coefficient, and the radiation mode amplifies heat transfer, while reducing the fanning friction coefficient. As wall emissivity increases from 0 to 1, effects of radiation on flow and thermal fields rise. However, there is no linear relationship for the whole range of ε. As scattering albedo varies between 0 and 0.75, radiation effects on flow and thermal fields for the constant and variable extinction coefficient are entirely opposite.

1. Introduction

Convective flow in channels has been of special interest over the past years, due to vast applications, such as solar collectors, electronic equipment, transistors and nuclear reactors. Some researchers have dealt with studies comprising combined multi-mode heat transfer. When convection and radiation are of similar importance, separate calculation of these two modes and superposition, without considering their interaction, can result in significant errors. Therefore, in high temperature channels, where a more accurate design and analysis is required, the momentum, energy and radiation transport equations should be solved simultaneously.

Although free, forced and mixed convection through vertical parallel plates has been studied abundantly [1–6], finding an exact analytical solution to the highly non-linear integro-differential Radiative Transfer Equation (RTE) is almost impossible. In the past decades, a variety of computational schemes has been developed to obtain an approximate solution to RTE, each having individual advantages in its application [7–10]. Fiveland [7,8] employed the S_n Discrete Ordinates Method (DOM) to find numerical solutions in two and three-dimensional enclosures with a gray, absorbing, emitting, isotropically and anisotropically scattering medium. His results have shown that the S_4, S_6 and S_8 solutions can be used for various surface and optical conditions to predict the radiant intensity and surface heat transfer. Combined radiative and conductive heat transfer in rectangular enclosures has been investigated by Kim and Baek [9]. The accuracy and efficiency of DOM, adopting its S_4 approximation, have been validated by comparing their numerical results for the non-scattering radiation–conduction problem, as well as the anisotropically scattering pure radiation problem, with other benchmark solutions, giving unanimous agreement. Also, they have reported

* Corresponding author.
E-mail address: bazdid@iust.ac.ir (F. Bazdidi-Tehrani).

Peer review under responsibility of Sharif University of Technology.

doi:10.1016/j.scient.2011.07.008

Nomenclature

a	absorption coefficient, m^{-1}
b	width of channel, m
D	width of channel in benchmark problem, m
f	local fanning friction coefficient
$\bar{f}$	total fanning friction coefficient
g	acceleration due to gravity, $m\ s^{-2}$
Gr	Grashof number, $= g\beta\Delta Tb^3/\nu^2$
i	intensity, $W\ m^{-2}\ sr^{-1}$
I	dimensionless intensity, $= i/\bar{\sigma}T_0^4$
I_b	dimensionless black body intensity
k	thermal conductivity, $W\ m^{-1}\ K^{-1}$
K	extinction coefficient, $= (a+\sigma)\ m^{-1}$
L	channel height, m
N	conduction–radiation parameter, $= kK/4\bar{\sigma}T_0^3$
n_x, n_y	number of cells in X and Y directions
p	pressure, Pa
P	dimensionless pressure, $(p - p_0/\rho v_0^2)$
Pe	Peclet number, =Re Pr
Pr	Prandtl number, $= \nu/\alpha$
Q_r	dimensionless radiative wall heat flux
Q_t	dimensionless total wall heat flux
Ra	Rayleigh number, =Gr Pr
Re	Reynolds number, $= v_0 b/\nu$
T	temperature, K
ΔT	temperature difference $= T_w - T_0$
u, v	velocity components in x and y directions, respectively, ms^{-1}
U, V	dimensionless velocity components in X and Y directions, respectively: $= ub/v$, $= v/v_0$
V_c	dimensionless axial centre-line velocity
w	weighting factor
x, y	coordinates in Cartesian system, m
X, Y	dimensionless coordinates in Cartesian system: $= x/b$, $= y/b$Re

Greek symbols

α	thermal diffusivity, $m^2\ s^{-1}$
β	thermal expansion coefficient, K^{-1}
ε	wall emissivity
θ	dimensionless temperature, $= (T - T_0)/(T_w - T_0)$
θ_b	bulk temperature, $= \int_0^1 V\theta dX$
μ, ξ	direction cosines
ν	kinematic viscosity, $m^2\ s^{-1}$
ρ	density, $kg\ m^{-3}$
σ	scattering coefficient, m^{-1}
$\bar{\sigma}$	Stefan–Boltzmann constant, 5.6697×10^{-8} $W\ m^{-2}\ K^{-4}$
τ	optical thickness, $= Kb$
ω	scattering albedo, σ/K
Ω	solid angle, sr
φ	phase function

Subscripts

m, m'	ordinate direction
0	inlet value
c	centre-line
x, y	coordinates directions in Cartesian system

that a reasonably short computational time is required to yield quite accurate solutions. Baek and Lee [10] then studied an unsteady two-phase radiation combined with conduction in a two-dimensional rectangular enclosure. They have used the DOM to solve the RTE, while the Finite Volume Method (FVM) is employed to resolve the energy equations for gas and particles. They have investigated the effects of particle and total absorption, extinction coefficient and wall emissivity on the time required to reach the steady-state condition. Conclusively, all these works have confirmed that the DOM has an acceptable capability to model the participating medium condition in radiation problems.

Meanwhile, studies addressing combined multi-mode heat transfer are relatively scarce. Combined thermal radiation and laminar forced convection with axial conduction and axial radiation in a circular pipe has been investigated by Yang and Ebadian [11]. They have modeled thermal radiation by the method of moments. Their study has demonstrated that the Peclet number is the first important parameter when considering the effects of axial conduction and axial radiation. Also, axial thermal radiation can safely be neglected when $Pe \times N > 50$. Yan and Li [12], numerically, and Krishnan et al. [13], experimentally, presented the effect of radiation on mixed convection heat transfer in vertical ducts. Combined mixed convection and radiation of an absorbing, emitting and scattering fluid in an inclined square duct has been investigated by Yan and Li [14], reporting that axial distributions of the fanning friction coefficient and Nusselt number are characterized by a drop near the duct inlet, due to the entrance effect. However, the decay is attenuated by the onset of secondary flow. Also, they have found that when the effect of radiation gets stronger, the extent of enhancement in the Nusselt number increases with a decrease in the conduction–radiation parameter.

Coupled convection–radiation heat transfer through parallel plates, with both heated and cooled walls, has been carried out by Talukdar and Simonson [15]. They have considered the flow as hydrodynamically and thermally developing, and reported that the axial radiation has a significant effect on the flow and thermal fields. Moreover, by assuming the flow as hydrodynamically developed, it can just reduce computing time and does not have a significant effect on results. Also, they have illustrated the effects of the extinction coefficient and wall emissivity on the Nusselt number and bulk temperature. Rao [16] has studied numerically the interaction of surface radiation with conduction and convection in a vertical channel with multiple discrete heat sources. The effect of Gr/Re on mixed convection and combined mixed convection–radiation heat transfer within a vertical channel, with variable wall temperature, has been investigated by Bazdidi-Tehrani and Nezamabadi [17]. They also solved the RTE using the DOM, adopting its S_4 quadrature scheme. They have reported that in the combined mixed convection–radiation case, the lower the ratio of Gr/Re, the less the variations of axial centre-line velocity from the beginning up to the end of the channel, and the more rapidly the fully developed flow will be attained.

Neither of the above works has paid attention distinctively to the occurrence of flow reversal. For a heated vertical channel, when the buoyancy parameter becomes large, the heated buoyant flow along the side wall becomes substantial. Depending upon the direction of the mainstream, the buoyant flow may cause different kinds of flow reversal, which can change the entire flow characteristics and enhance heat transfer in different manners. Flow reversal, as a significant phenomenon in ducts,

is conducted by some researchers [18–20]. Barletta [21,22] analytically investigated this phenomenon occurring under the fully developed conditions for mixed convection in a vertical duct. He has also analyzed flow reversal affected by a choice of boundary conditions, showing that it takes place near the cold wall, while the walls are heated asymmetrically. Ingham et al. [23] have studied numerically the occurrence of flow reversal for mixed convection in vertical and ducts with no consideration of radiation. Furthermore, Desrayaud and Lauriat [24] have numerically demonstrated the occurrence of flow reversal in laminar mixed convection flow in the entry region of symmetrically heated walls, and they have displayed that the vertical channel length has no influence on the occurrence of reversed flow when $L/D > 10$.

Radiative parameters also have a significant role to play in the occurrence of flow reversal in mixed convective flows. Bazdidi-Tehrani and Shahini [25] investigated numerically the effects of two radiative parameters, namely, the conduction–radiation parameter and optical thickness, on the occurrence of flow reversal within a vertical constant wall temperature channel. Their results have displayed that when the radiation effects increase, the occurrence of flow reversal is postponed to the higher values of Gr/Re.

As mentioned above, the influence of extinction coefficient, K, on flow and thermal fields, particularly on the Nusselt number and bulk temperature, has been presented by Talukdar and Simonson [15]. They have assumed that while K alters the other radiative parameters, N and τ are not constant. Therefore, the effects of radiative properties, such as absorbing and scattering, on the flow and thermal fields have not been made distinctively clear. However, scattering albedo, ω, is based on the absorption coefficient and scattering coefficient, each of which has its own particular effect on the RTE. In previous studies, the effects of these two parameters have not been addressed separately. This has motivated the present work to pay particular attention to the effects of absorption and scattering coefficients on the flow and thermal fields and in particular on the occurrence of flow reversal.

In addition, in mixed convection, the occurrence of reversed flow increases the amount of heat transfer between the mainstream and walls [24]. On the other hand, it causes a growth in the fanning friction coefficient [26]. Hence, this issue should be particularly noticed in order to find the optimum design in a practical design situation. Even though the effect of radiation parameters, such as K and ε, on the Nusselt number and bulk temperature has received attention recently [15], the influence of the presence of both thermal radiation and flow reversal on the fanning friction coefficient in mixed convection flows has drawn no attention. Hence, it will be addressed in detail in the present work.

In continuation of previous work [25], the objective of the present paper is to deal with the numerical analysis of a combined mixed convection–radiation heat transfer problem within symmetrically heated vertical parallel plates, where the radiation effects (i.e., emitting, scattering and absorbing) have been considered both for walls and the participating medium. Thus, a home-made CFD code is developed to investigate the influence of two radiative parameters, namely, wall emissivity, ε, and scattering albedo, ω, while the extinction coefficient is kept either constant or not (i.e., K varies by changing the scattering coefficient, and it represents the reality of ω variations, which is not addressed in the previous work of [12,15]) on the occurrence of flow reversal, fanning friction coefficient, flow and thermal fields extensively.

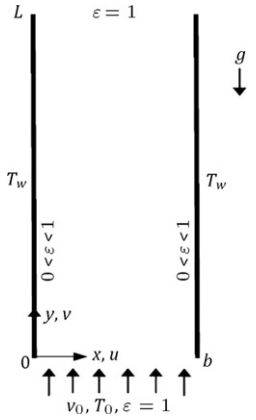

Figure 1: Schematic view of the vertical parallel-plates channel and the boundary conditions.

2. Mathematical formulation and calculation procedure

The physical model and boundary conditions under consideration, as illustrated in Figure 1, consist of a two-dimensional channel of width, b. Channel walls, as two vertical parallel plates, are maintained at a temperature, T_w, greater than the temperature, T_0, of the inlet fluid. The channel is open at both ends and the fluid entering from the bottom has uniform v_0. The flow is both thermally and hydrodynamically developing. The working fluid is taken to be air, with constant $\mathrm{Pr} = 0.71$, and the flow is assumed to be incompressible, laminar and two-dimensional. Also, viscous dissipation is regarded as negligible.

The axial conductive heat transfer in the channel walls is neglected. All thermodynamic properties of the fluid are taken as constant, except the density in the buoyancy term in the y-momentum equation. The variation of density follows the Boussinesq approximation [1], as follows:

$$\rho = \rho_0[1 - \beta(T - T_0)]. \tag{1}$$

The channel walls are considered as diffuse-gray surfaces, and the inlet and outlet of the channel are assumed as imaginary surfaces, with $\varepsilon = 1$. The participating medium is assumed as Newtonian, incompressible and gray, comprising all the radiative properties (i.e., absorbing, emitting, and scattering), where the scattering is isotropic and the phase function (φ) is assumed to be 1.

For the numerical solution of equations, first the following dimensionless parameters are defined:

$$\begin{aligned}
&X = x/b, \quad Y = y/b\,\mathrm{Re}, \quad U = ub/v_0,\\
&V = v/v_0, \quad \theta = (T - T_0)/(T_w - T_0),\\
&\Delta T = T_w - T_0, \quad P = (p - p_0)/\rho v_0^2,\\
&\mathrm{Re} = v_0 b/v, \quad \mathrm{Gr} = g\beta\Delta T b^3/v^2,\\
&\mathrm{Pr} = v/\alpha, \quad I = i/\bar{\sigma}T_0^4, \quad N = kK/4\bar{\sigma}T_0^3,\\
&\omega = \sigma/K, \quad \tau = Kb, \quad K = a + \sigma.
\end{aligned} \tag{2}$$

The governing equations and boundary conditions are expressed in a dimensionless form as follows:

conservation of mass:

$$\frac{\partial U}{\partial X} + \frac{\partial V}{\partial Y} = 0, \tag{3}$$

conservation of transverse and axial momentum:

$$U\frac{\partial U}{\partial X}+V\frac{\partial U}{\partial Y}=-\mathrm{Re}^2\frac{\partial P}{\partial X}+\frac{\partial^2 U}{\partial X^2}+\frac{1}{\mathrm{Re}^2}\frac{\partial^2 U}{\partial Y^2}, \tag{4}$$

$$U\frac{\partial V}{\partial X}+V\frac{\partial V}{\partial Y}=-\frac{\partial P}{\partial Y}+\frac{\partial^2 V}{\partial X^2}+\frac{1}{\mathrm{Re}^2}\frac{\partial^2 V}{\partial Y^2}+\frac{\mathrm{Gr}}{\mathrm{Re}}\theta, \tag{5}$$

conservation of energy:

$$U\frac{\partial \theta}{\partial X}+V\frac{\partial \theta}{\partial Y}=\frac{1}{\mathrm{Pr}}\left\{\frac{\partial^2\theta}{\partial X^2}+\frac{1}{\mathrm{Re}^2}\frac{\partial^2\theta}{\partial Y^2}+Sr\right\}, \tag{6}$$

$$\mu\frac{\partial I}{\partial X}+\xi\frac{1}{\mathrm{Re}}\frac{\partial I}{\partial Y}=-\tau I+\frac{\tau}{4\pi}\left[4(1-\omega)\left(\frac{T}{T_0}\right)^4+\omega\int_0^{4\pi} I\,\mathrm{d}\Omega\right]. \tag{7}$$

The last term in Eq. (6) signifies the radiative energy source, which is obtained from the Radiative Transfer Equation (RTE) [27], as presented by Eq. (7). The three right-hand-side terms represent the changes in intensity, due to absorption and out-scattering, emission and in-scattering, consecutively. The Re parameter is produced in the process of the nondimensionalization of governing equations.

The boundary conditions for the present problem are defined as follows:

$$\begin{aligned}
&\text{At } 0<X<1,\ Y=0:\\
&\quad U=0,\qquad V=1,\qquad \theta=0,\qquad \varepsilon=1,\\
&\text{At } X=0,\ Y>0:\\
&\quad U=0,\qquad V=0,\qquad \theta=1,\qquad 0\le\varepsilon\le 1,\\
&\text{At } X=1,\ Y>0:\\
&\quad U=0,\qquad V=0,\qquad \theta=1,\qquad 0\le\varepsilon\le 1,\\
&\text{At } 0<X<1,\ Y=L/b\,\mathrm{Re}:\\
&\quad P=0,\qquad \partial\theta/\partial Y=0,\qquad \varepsilon=1.
\end{aligned} \tag{8}$$

In the present work, the radiative transfer equation (7) is solved by using the Discrete Ordinates Method (DOM), adopting its S_6 quadrature scheme [7]. This method is described, in detail, by Siegel and Howell [27]. The solid angle, 4π, is discretized over a finite number of directions and the RTE is applied to these directions, with the integral term replaced by a quadrature. The discrete ordinates representation of the RTE is:

$$\mu_m\frac{\partial I_m}{\partial X}+\xi_m\frac{1}{\mathrm{Re}}\frac{\partial I_m}{\partial Y}=-\tau I_m+\frac{\tau}{4\pi}\left[4(1-\omega)\left(\frac{T}{T_0}\right)^4+\omega\sum_{\mu_{m'}<0}\mu_{m'}w_{m'}I_{m'}\right]. \tag{9}$$

Boundary conditions for the RTE:

$$\begin{aligned}
&\text{Left wall}\quad \mu_m>0,\\
&I_m=\varepsilon+\frac{1-\varepsilon}{\pi}\sum_{\mu_{m'}<0}w_{m'}\,|\mu_{m'}|\,I_{m'},\\
&\text{Right wall}\quad \mu_m<0,\\
&I_m=\varepsilon+\frac{1-\varepsilon}{\pi}\sum_{\mu_{m'}>0}w_{m'}\mu_{m'}I_{m'},\\
&\text{Inlet}\qquad I_m=1,\\
&\text{Outlet}\qquad I_m=1.
\end{aligned} \tag{10}$$

In the above equations, the values, m and m', denote outgoing and incoming directions, respectively; w is a weighing factor, and ε is the wall emissivity assumed to be unity for both walls.

The finite volume-based finite difference method, together with the well-known SIMPLE algorithm of Patankar [28], is employed for solving the simultaneous governing equations (3)–(6), along with the relevant boundary conditions. The radiative transfer equation is integrated over a 2D control volume, and to make the relation between boundary intensities and upstream nodal intensities, the step scheme [27] is used.

The Grashof number to Reynolds number ratio, Gr/Re, is one effective parameter in the study of mixed convective flows, which has been widely used previously [17–25]. Also, it has been found that the flow reversal takes place when Gr/Re surpasses a threshold value. Consequently, this ratio is used as a flow parameter to particularly investigate the occurrence regime of flow reversal corresponding to radiative parameters. Gr/Re usually varies between 400 and 2000, and this is a safe range to study the onset of flow reversal presently under investigation.

2.1. Grid sensitivity analysis

To ensure the independence of the present grid points, a test is made on the grids in the transverse and axial step size. Grids are arranged to be uniform in the axial direction but non-uniformly distributed in the transverse direction, because of wall effects imposed by velocity and thermal boundary layers.

In order to show that the present results are independent of mesh size, eight different mesh sizes are examined, as depicted in Table 1. By approaching the reference grid size (i.e. 23 × 152) from lower and higher levels in both stream-wise and transverse directions, it is observed that the percentage of deviations in the centre-line velocity and temperature descend, and when one moves far from the reference grid size, a significant difference between the results is obtained. Hence, the mesh size of 23 × 152 is regarded as the optimum and is adopted throughout the present study. For the solution of RTE, the same mesh sizes are adopted and there is no need to create new meshes.

Eqs. (3)–(8) are solved through an iterative procedure. The relevant convergence criteria presently employed are defined as follows:

$$\begin{aligned}
&\max\left|\frac{V_{i+1}-V_i}{V_i}\right|<5*10^{-7},\\
&\max\left|\frac{\theta_{i+1}-\theta_i}{\theta_i}\right|<5*10^{-7},
\end{aligned} \tag{11}$$

where i and $i+1$ denote two successive iterations in the solving procedure.

3. Results and discussion

In the present work, the influence of two radiative parameters, namely, wall emissivity, ε, and scattering albedo, w, while the extinction coefficient is kept either constant or not, on the occurrence of flow reversal, fanning friction coefficient, flow and thermal fields, is studied.

3.1. Numerical model validation

To validate the accuracy of the present numerical model, two direct comparisons are made between the present data

Table 1: Comparison of centre-line velocity and temperature at $Y = 0.2$ for various grids (Gr/Re $= 1000$, $N = 0.4$, $\tau = 0.25$, $\omega = 0.5$, $\varepsilon = 0.5$).

Number	$nx \times ny$	V_c	Deviation from Ref. grid (%)	θ_c	Deviation from Ref. grid (%)
1	23 × 76	1.032739821	1.15	0.933571138	0.52
2	23 × 100	1.036834836	0.76	0.935704498	0.3
3	23 × 152	1.044829547	–	0.938482278	–
4	23 × 200	1.031026304	1.32	0.937356116	0.12
5	23 × 300	1.003051937	4	0.940653364	0.23
6	33 × 152	1.017663978	2.6	0.940359242	0.2
7	43 × 152	1.014529490	2.9	0.940453091	0.21
8	43 × 350	1.012439831	3.1	0.940546939	0.22

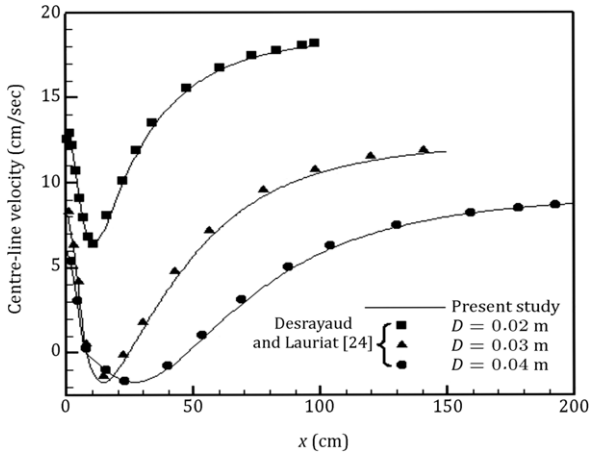

Figure 2: Variation of axial centre-line velocity with channel height for three values of channel width, D.

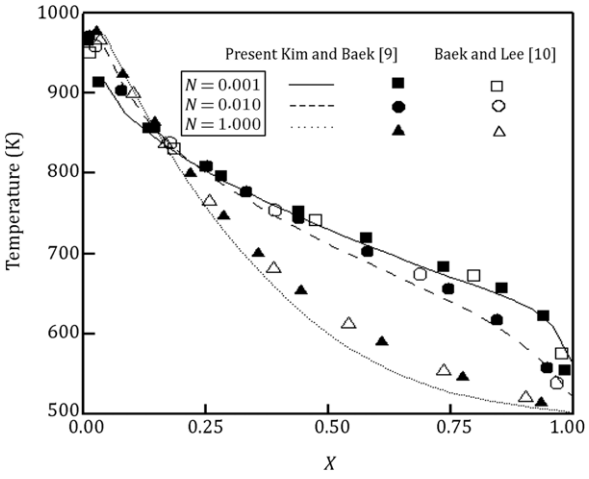

Figure 3: Comparison of mid-plane temperature profiles ($Y = 0.5$) for various conduction–radiation parameters, N.

and those available in the literature. Firstly, the streamwise variation of the centre-line axial velocity versus the duct height (see Figure 2) is compared with the finite volume solution related to the flow reversal of laminar mixed convection in the entry region of symmetrically heated vertical plate channels, as presented by Desrayaud and Lauriat [24]. Comparisons are carried out at Re $= 300$ and $L/D = 50$ for three values of Gr as 4.71×10^4, 1.6×10^5 and 3.77×10^5, corresponding to channel width, D, equal to 0.02, 0.03 and 0.04 m, respectively. It can be seen that the present results agree well with those available from Ref. [24] and the overall deviation is less than 4% on average. Furthermore, it is clear that the flow reversal takes place when Gr increases with a growth of D.

Secondly, to verify the present subroutine developed for solving the RTE, the DOM is applied to a two-dimensional rectangular enclosure with black walls containing an absorbing and emitting medium. The left wall temperature is kept constant at $T = 1000$ K and the others are at $T = 500$ K ($\tau = 1$, $\omega = 0$, $\varepsilon = 1$, $N = 0.001$, 0.01 and 1). Figure 3 represents the temperature variations of the working fluid with X at the mid-plane ($Y = 0.5$) for various conduction–radiation parameters, N, and the present results are compared with those of Kim and Baek [9] and Baek and Lee [10]. Although there is a difference, particularly for $N = 1$ at $0.4 < X < 0.8$, the agreement is acceptable and the overall deviation is less than 7% on average.

The present results are illustrated as the profiles of centre-line velocity, streamlines, the occurrence regime of flow reversal, fanning friction coefficient, radiative and total wall heat fluxes and bulk temperature for various values of the radiative parameters in the following sections. The parameters that are kept fixed are: $\frac{T_0}{\Delta T} = \frac{1}{2}$, Pr $= 0.71$ and $\frac{L}{b} = 14$.

The local and averaged fanning friction coefficients are defined as in Eq. (12).

$$f\mathrm{Re} = 2\frac{\partial U}{\partial Y}\bigg|_{x=0}, \qquad \bar{f}\mathrm{Re} = \frac{2}{A}\int_0^A \frac{\partial U}{\partial Y}\bigg|_{x=0} \mathrm{d}X. \tag{12}$$

The non-dimensional forms of Q_r and Q_t, the latter comprising both conduction and radiation modes, are defined as follows:

$$Q_r = \sum_{m'} \mu_{m'}\omega_{m'}I_{m'}, \tag{13}$$

and:

$$Q_t = Q_r - \frac{4}{N\tau}\frac{\Delta T}{T_0}\frac{\partial \theta}{\partial X}\bigg|_{x=0}. \tag{14}$$

The bulk temperature, θ_b, is defined by Eq. (15):

$$\theta_b = \int_0^1 V\theta \mathrm{d}X. \tag{15}$$

3.2. Variation of wall emissivity, ε

One of the most important parameters in radiation heat transfer is emissivity, ε. Among all radiative properties in a channel, ε belongs to the walls, and the rest (N, τ and ω) are for the participating medium. It specifies how well a real body radiates energy, as compared with a black body. Wall emissivity varies between 0 and 1. A larger value of ε indicates a larger radiative heat flux, which is emitted by the walls, which behave like a black body when $\varepsilon = 1$. Increasing ε means a greater effect of radiation mode on thermal and flow fields. In this

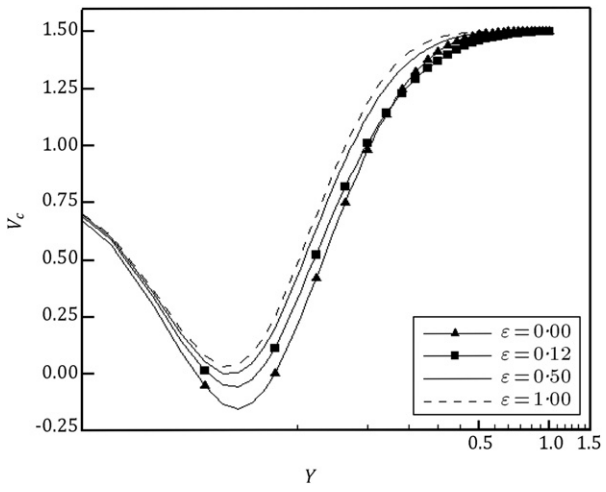

Figure 4: Variations of axial centre-line velocity with channel height for various values of ε.

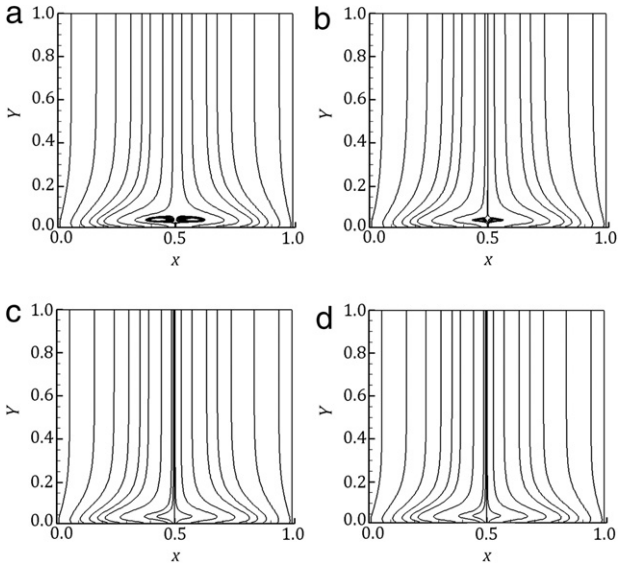

Figure 5: Streamlines for various values of ε. (a) $\varepsilon = 0$; (b) $\varepsilon = 0.12$; (c) $\varepsilon = 0.5$; and (d) $\varepsilon = 1$.

section, the effect of wall emissivity is investigated under the following typical assumptions of Gr/Re $= 1000$, $N = 0.4$, $\tau = 0.25$ and $\omega = 0.5$.

According to Figure 4, at the channel entrance ($0.03 < Y < 0.06$) near the wall, due to the presence of the buoyancy force, axial velocity is enhanced. Since the flow rate at any cross section is constant, satisfying the mass conservation law, the velocity at the centre of the channel is a minimum. Under special circumstances, the axial velocity becomes negative, which is regarded as 'flow reversal'. This phenomenon is discussed, in detail, in the following parts. One of the parameters employed to show this phenomenon is the centre-line velocity. In Figure 4, the influence of ε on the centre-line velocity, at constant Gr/Re, is presented. It can be observed that for the no radiation condition, including $\varepsilon = 0$ and when $\varepsilon = 0.12$, the centre-line velocity is negative at the channel entrance region. It means that flow reversal occurs and the fluid is rotating at the centre of the channel. Another noticeable point is that when ε increases towards 1 (i.e., as the effect of radiation increases), the profile of the centre-line velocity approaches its fully developed condition more rapidly.

Figure 5 depicts the streamlines for various values of ε, in the range of 0–1. In line with the above-mentioned statement, streamlines demonstrate that when the radiation effects are negligible or they have a minor effect ($\varepsilon \leq 0.12$), a recirculation cell is observed at the centre-line near the entrance of the channel, which is because of a moderate difference between wall and inlet flow temperatures. This difference creates a large buoyancy force in the vicinity of the walls, which accelerates flow in the upward direction. When this acceleration is high, the centre-line velocity force is negative and hence the recirculation cell is produced and the streamlines are squeezed near the wall.

Also, when the radiation effects grow by increasing ε ($\varepsilon \geq 0.5$), mixed convection loses its power, since the radiation makes a uniform temperature distribution across the channel width. As a result, while ε reaches 0.5, the shape of cells is changed, although the size of the recirculation region is reduced and is finally vanished. After that, when ε increases to 1, streamlines do not undergo a considerable change. In Figure 5a, where $\varepsilon = 0$, recirculation cells have their largest size and, when $\varepsilon \geq 0.5$ (Figure 5c and d), the recirculation cell is completely vanished.

As discussed in past literature, natural convection always increases the rate of heat transfer and hence mixed convection has a higher thermal efficiency in comparison with forced convection in the same range of Re [12,24]. In addition, it should be noticed that although the Nusselt number is an important parameter in the evaluation of a thermal system, it is unjust to neglect the effects of the fanning friction coefficient in practical design situations. Radiation mode increases the value of the bulk temperature, although it makes the temperature distribution uniformly across the channel width [25], meaning that the effect of the buoyancy force reduces by the growth of radiative effects. Since the fanning friction coefficient is related to the flow field, which is moderately affected by the buoyancy force in mixed convective flows, this opposite treatment of radiation and natural convection concerning the fanning friction coefficient contains some interesting points, which are presented in the following parts. Therefore, in the present study, variation of this parameter is evaluated for various values of the radiation parameters, namely, wall emissivity and scattering albedo.

Figure 6 illustrates the variation of fanning friction coefficient, fRe, with the channel height, for a wide range of ε. The linear sharp drop in fRe at the entrance section of the channel is due to the developing hydrodynamic and thermal boundary layers. It then increases slightly, reaching a peak, and then again decreases exponentially until it approaches a constant value ($=11.918$) under the fully developed condition. The value of 11.918 refers to the pure forced convection flow. The fanning friction coefficient in both mixed and forced convective flows reaches a constant value under the fully developed conditions.

Clearly, in the mixed convection flow, fRe has a larger value as compared with the pure forced convection [12,14,22]. Although this coefficient is reduced by increasing the radiation effects, it never reaches the range of pure forced convection [12,14]. According to Figure 6, after a sharp decrease at the entrance region, fRe reaches a peak, which refers to the squeezing of streamlines to the walls (see Figure 5a and b). It means that flow reversal makes this coefficient larger than before [26] and the radiation mode not only raises the rate of heat transfer but also reduces the fanning friction coefficient [12,14].

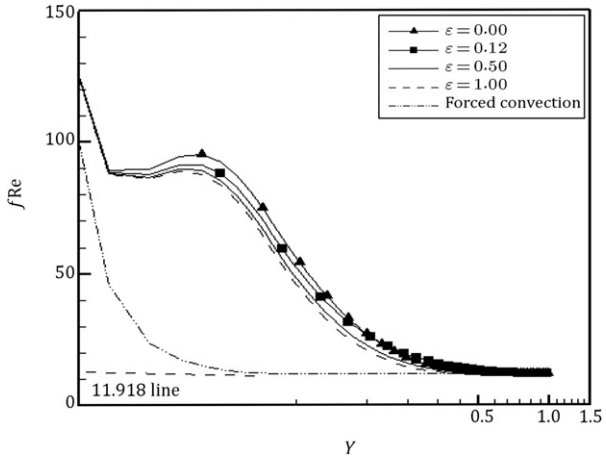

Figure 6: Variation of fanning friction coefficient with channel height for various values of ε.

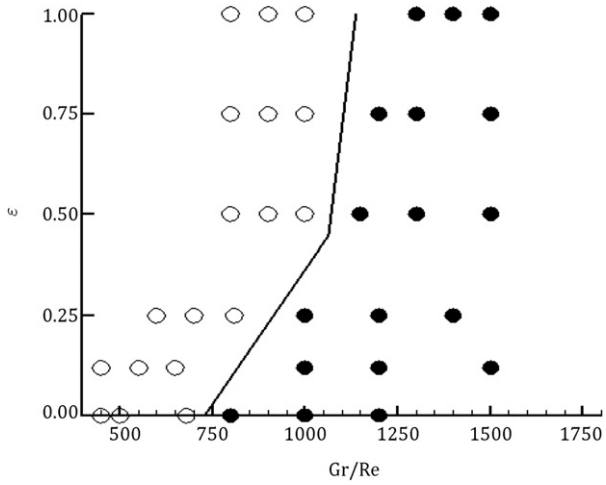

Figure 7: Flow reversal occurrence regime ($N = 0.4, \omega = 0.5, \varepsilon = 0.5$).

Figure 7 shows the effect of wall emissivity on the occurrence of flow reversal for a wide range of Gr/Re, while the other radiation parameters are fixed. The bold symbols represent the conditions at which flow reversal happens. It is observed that as ε increases, the threshold value of Gr/Re for flow reversal occurrence increases from approximately 700 to 1200. It demonstrates the significant influence of radiation on the distribution of heat energy through the channel, which results in avoiding an occurrence of flow reversal. It should, however, be noticed that there is no linear relationship for the whole range of ε. For instance, as ε increases from 0 to 0.5, the value of critical Gr/Re changes approximately from 700 to 1100, and when ε rises from 0.5 to 1, it just changes from 1100 to 1200.

Figure 8 illustrates the variations of radiative and total wall heat fluxes, Q_r and Q_t, versus the channel height for various values of ε and at a fixed Gr/Re =1000. For the total heat flux, the condition of no radiation is also displayed. It should be mentioned that Q_r is obtained by the summation of incoming and outgoing radiative wall heat fluxes. The radiative flux that reaches the wall from the inlet surface, outlet surface, opposite wall and fluid is considered as the incoming flux, and the radiative flux emitted and reflected from the wall is considered as the outgoing flux. For all values of ε, at a height greater than $Y = 0.75$, Q_r is almost zero, which implies the equality of the incoming and outgoing radiative heat fluxes. It is shown that the radiative and total heat fluxes are affected by the variation of ε. Also, there is a considerable change in Q_r when ε varies from 0 to 0.5, and this change is not however noticeable as ε alters from 0.5 to 1. As a result, there is no linear relationship between the occurrence of flow reversal and variation of ε for the whole range of ε.

Figure 8 also implies that for all values of ε, Q_t is greater than Q_r, due to the addition of the conduction heat flux to the radiation flux. At the entrance region of the channel, due to the steep gradient of the temperature near the wall, the conduction heat flux is significantly greater than the other sections throughout the channel wall and thus the difference between Q_t and Q_r is remarkable.

Figure 9 shows the variations of bulk temperature with the channel height for various values of ε, including the no radiation condition. When the radiation mode is stronger, the bulk temperature reaches its maximum value rapidly. It means that as ε increases, the fluid flow reaches its thermally developed state more rapidly. This is because the radiation is an extra mode of heat transfer that makes the energy more distributed.

3.3. Variation of scattering albedo, ω

Scattering albedo is a known variable in radiation heat transfer. Scattering is the redirection of radiation by the interaction with particles or molecules within the medium. Scattering albedo represents the ability of scattering to attenuate the intensity of radiation [27] (see Eq. (7)). In the present work, the variation of ω in the range of 0 to 1 is investigated, while the conduction–radiation parameter, N, is constant. Therefore, we have two choices: the first one is a constant extinction coefficient, K, and the second is a variable extinction coefficient.

Scattering coefficient, σ, may be varied to change the value of ω, while K is constant (i.e., $a+\sigma$ = constant) and the absorption coefficient, a, has to alter. In this case, optical thickness, τ, is kept fixed (i.e., $\tau = 0.25$). For instance, when σ increases, a has to reduce and therefore the medium absorbs less energy from the radiative heat flux. The outcome of this process is discussed in the following parts. As for the second choice, a does not need to vary and is kept constant. In this situation, τ varies between 0.125 and 0.5, giving the following values for ω: $\omega = 0$ and $\tau = 0.125$, $\omega = 0.5$ and $\tau = 0.25$ and $\omega = 0.75$ and $\tau = 0.5$. The effects of τ variation have been discussed previously [25].

By assuming constant K, a larger value of ω is resulted, meaning that a higher amount of radiation is scattered and only a little passes through the medium. Also, less energy is absorbed by the medium. Hence, the radiation mode is not so effective. Also, when ω is 0, the participating medium does not decrease radiation effects. Although ω varies between 0 and 1, significant effects take place in the larger values. This is discussed further in the following sections. However, for the variable K condition, the treatment of radiation is changed entirely and, in the present study, the variations are shown in detail. In this section, the effect of scattering albedo is studied under the assumptions of Gr/Re = 1000, $N = 0.4$ and $\varepsilon = 0.5$.

Figure 10 depicts the present variations of axial centre-line velocity with channel height, for different values of ω, at a constant Gr/Re. For the constant K condition, as ω increases toward 1, the minimum centre-line velocity lessens, so that for $\omega = 0.75$ and also for the no radiation condition of $\omega = 1$, flow reversal takes place. When K is not constant, reversed flow

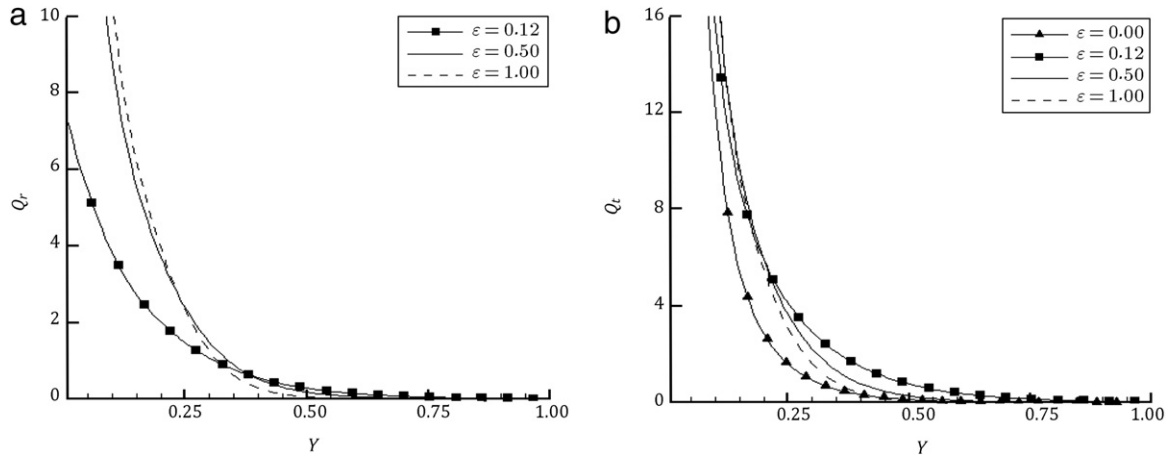

Figure 8: Variations of radiative and total wall heat fluxes with channel height for various values of ε.

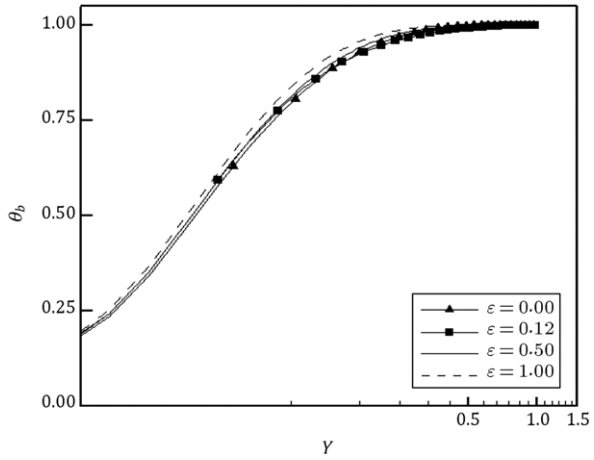

Figure 9: Variation of bulk temperature with channel height for various values of ε.

occurs at both $\omega = 0$ and $\omega = 1$. Also, it can be seen from Figure 10a that the effect of radiation increases when ω grows from 0 to 0.75, and the minimum centre-line velocity increases during this change. This is due to the fact that with an increase in K, by an increase of σ, the influence of radiation as an additional mode is enhanced, and the radiation flux can reach the centre-line of the channel.

Figure 11 demonstrates the streamlines for various values of ω at a constant Gr/Re. For the constant K (left column), for the lowest value of $\omega = 0$, implying that the radiation is effective, energy is more distributed through the medium and the results show no recirculation region. Also, streamlines indicate that when the radiation effects are neglected or of a minor effect, such as for $\omega = 0.75$ and 1, a recirculation cell is observed at the centre-line near the entrance of the channel. For the variable K condition (right column), as discussed in Figure 10 for the centre-line velocity, the presence of the radiation mode alters the shape of the recirculation region and reduces the cells size when ω is increased from 0 to 0.75. After that, the recirculation region is produced again for the no radiation condition of $\omega = 1$ and the flow reversal takes place. It can be concluded that the influence of scattering albedo on the occurrence of flow reversal for the constant K condition is not similar to the variable K.

Figure 12 shows the variation of fanning friction coefficient, fRe, with the channel height for a wide range of ω. The overall trends for both constant K and variable K conditions are the same, which is quite similar to the variation of fRe for various values of ε, as discussed previously in Figure 6. The interesting behavior is the slight increase, which is the result of the buoyancy force squeezing the streamlines to the walls. For

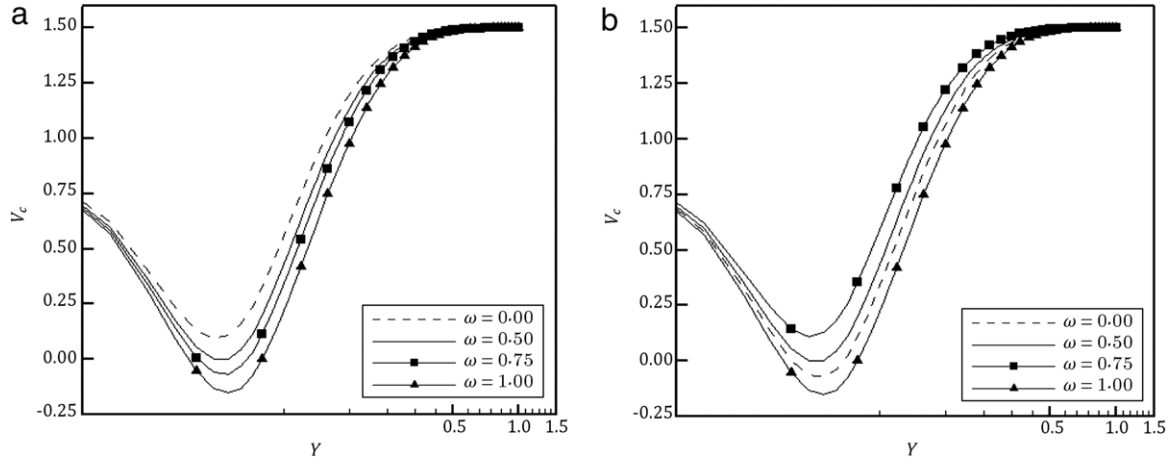

Figure 10: Variations of axial centre-line velocity with channel height for various values of ω; (a) K is constant, $\tau = 0.25$; and (b) K is variable, $0.125 \leq \tau \leq 0.5$.

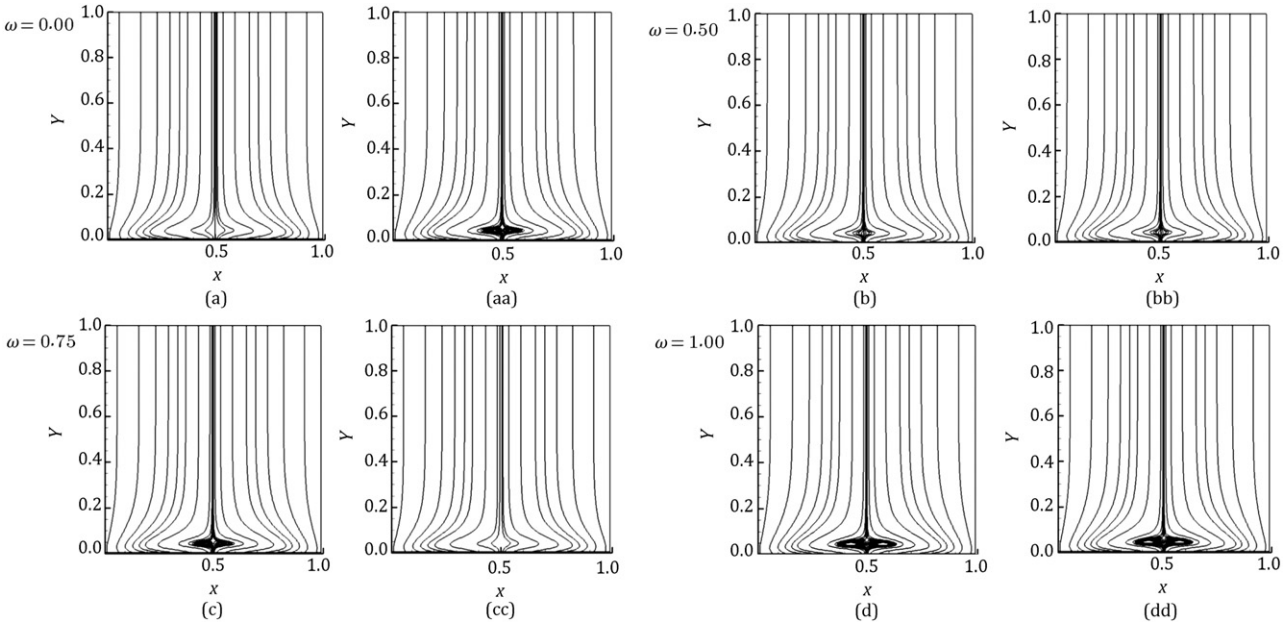

Figure 11: Streamlines for various values of ω; Left column: K is constant, $\tau = 0.25$ and Right column: K is variable, $0.125 \leq \tau \leq 0.5$.

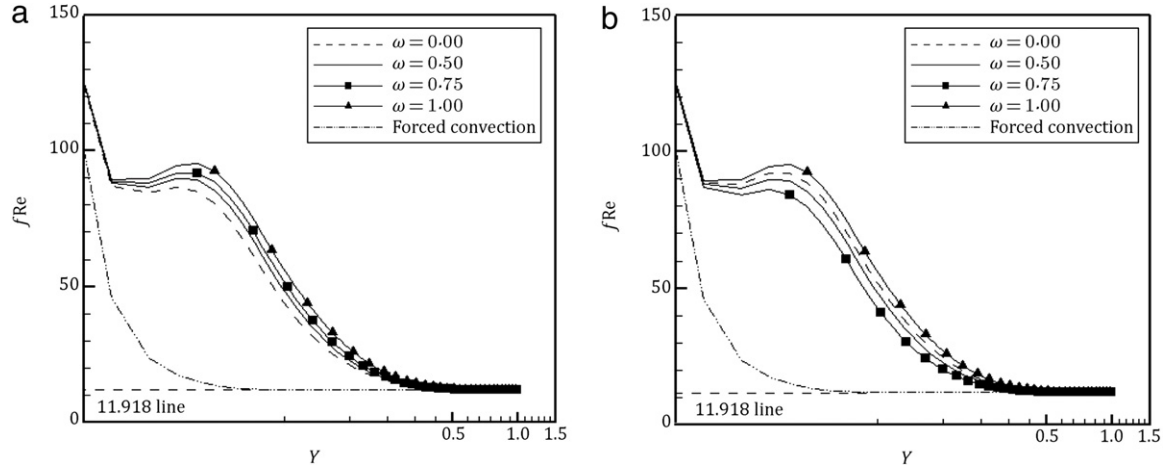

Figure 12: Variation of fanning friction coefficient with channel height for various values of ω. (a) K is constant, $\tau = 0.25$; and (b) K is variable, $0.125 \leq \tau \leq 0.5$.

constant K, $f\mathrm{Re}$ is reduced by a decrease of scattering albedo due to the reduction of the buoyancy force effect. For variable K, it is observed that while scattering coefficient, σ, increases, $f\mathrm{Re}$ decreases for $0 \leq \omega \leq 0.75$ and then increases for $0.75 < \omega \leq 1$ reaching its peak.

Figure 13 depicts the influence of ω variations on the occurrence regime of flow reversal for a wide range of Gr/Re, while the conduction–radiation parameter, N, is constant. The bold symbols represent the conditions under which flow reversal occurs. From Figure 13a, as ω decreases, the threshold value of Gr/Re for flow reversal occurrence increases, when K is constant. It demonstrates the significant effect of radiation on the distribution of heat energy through the channel, which results in avoiding the occurrence of flow reversal. For the variable K condition (Figure 13b), the behavior is on the contrary. That is as ω decreases from 0.75 to 0, the occurrence of reversed flow takes place in smaller Gr/Re. Also, while ω increases from 0.75 to 1, the threshold value of Gr/Re is reduced moderately from 1300 to 700.

Figure 14 represents the radiative and total wall heat fluxes, Q_r and Q_t, along the channel height for various values of ω. For all values of ω at a height greater than $Y = 0.6$, Q_r and Q_t are approximately zero, meaning that equality exists between the incoming and outgoing radiative and total heat fluxes. When K is constant, for all values of ω, the radiative and total heat fluxes are generally the same and do not change by any variation of ω. This is because when ω varies between 0 and 1, σ is changed. But it should be noticed that a has to be changed to keep N as a constant parameter. Therefore, when scattering increases, absorption decreases too, and vice versa. Thus, Q_r does not change for various values of ω. For variable K, Figure 14 indicates a slight growth in Q_r and also a moderate increase in Q_t as ω is reduced from 1 to 0. This is due to the fact that with an increase in ω, the effect of radiation as an additional mode is decreased and less transfer of energy occurs between the fluid and the walls.

Figure 15 represents the variations of bulk temperature along the channel height for different values of ω and for a constant Gr/Re. The results for the no radiation condition ($\omega = 1$)

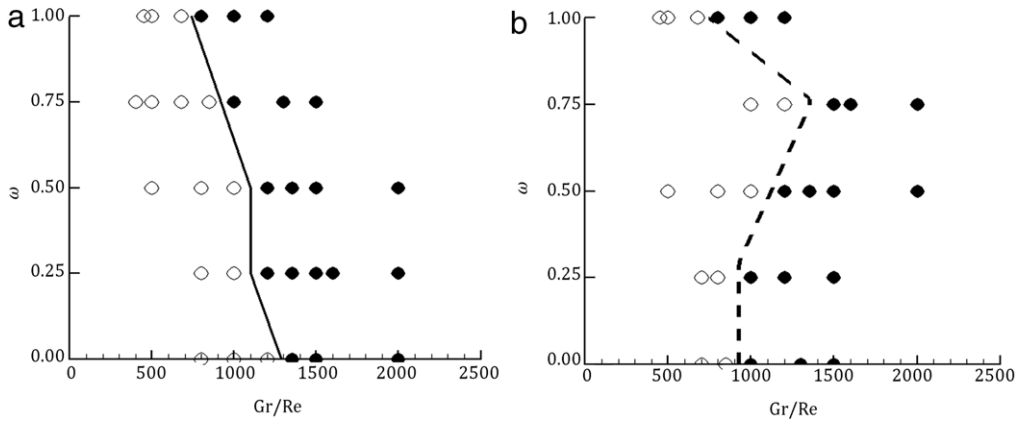

Figure 13: Flow reversal occurrence regime. (a) K is constant, $\tau = 0.25$, and (b) K is variable, $0.125 \leq \tau \leq 0.5$ ($N = 0.4$, $\varepsilon = 0.5$).

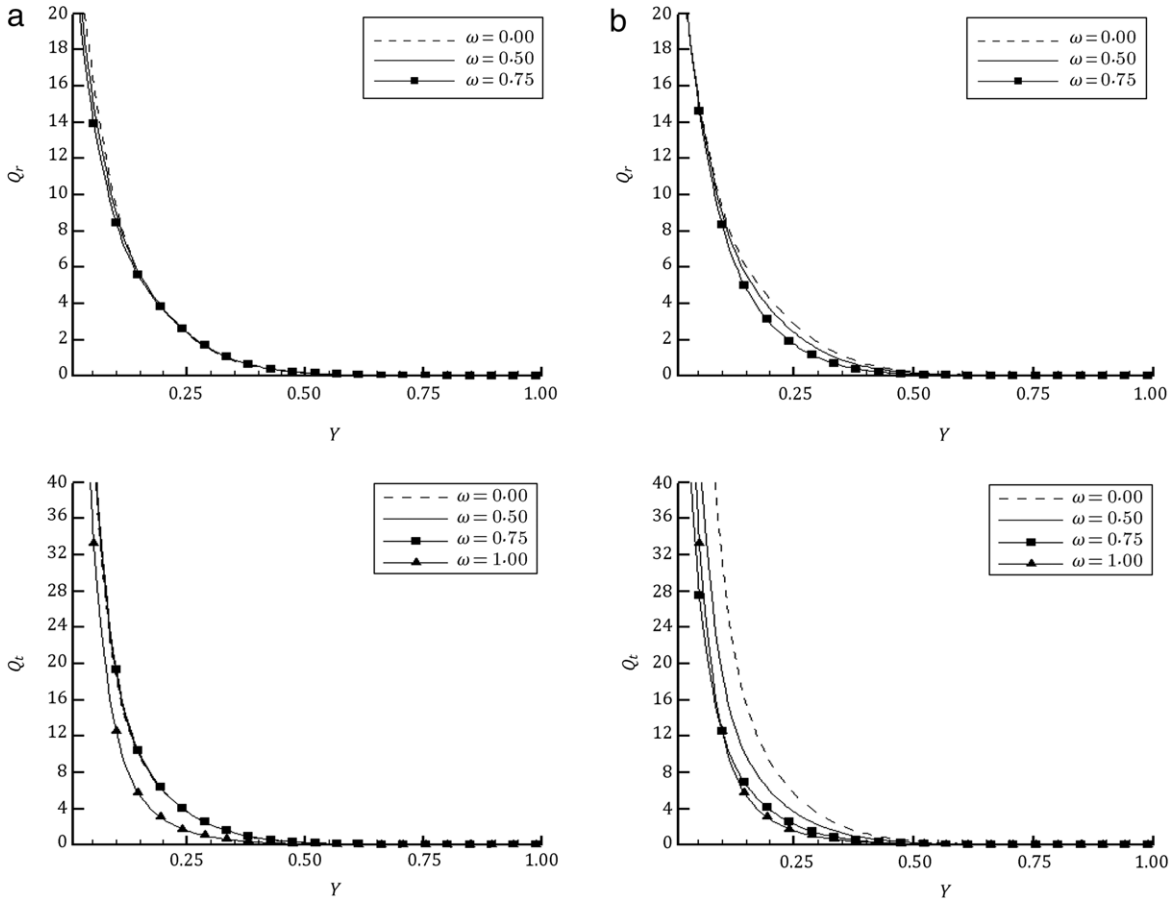

Figure 14: Variations of radiative and total wall heat fluxes with channel height for various values ω. (a) K is constant, $\tau = 0.25$; and (b) K is variable, $0.125 \leq \tau \leq 0.5$.

illustrate that there is a slight growth in the variation of bulk temperature, as compared with the case of $\omega = 0$. Moreover, for lower values of ω, the bulk temperature approaches its maximum more rapidly. It means that with a decrease in ω, similar to the increase in ε presented in Figure 9, the fluid flow reaches its thermally developed state more quickly.

4. Conclusions

The main objective of the present work is to investigate the influence of two important radiative parameters, namely, scattering albedo and wall emissivity, on the occurrence of buoyancy-assisted flow reversal, flow and thermal fields. The main points may be concluded as follows:

1. As ε increases, fluid flow reaches its hydrodynamically and thermally developed state more rapidly. Also, it causes the fanning friction coefficient to have a lower value.
2. The radiative wall heat flux and total heat flux are significantly affected, while ε varies between 0 and 0.5. As ε increases, the bulk temperature increases more quickly and reaches the wall temperature.

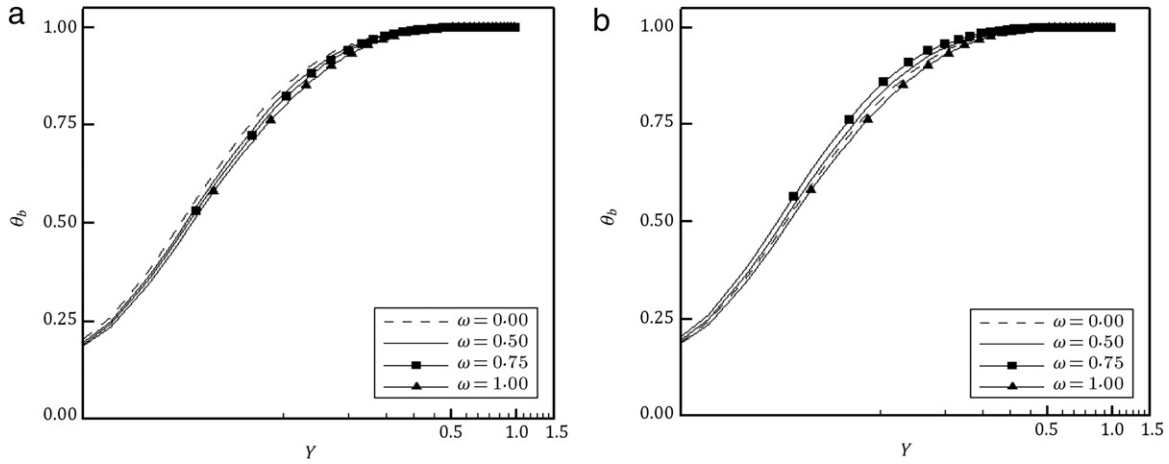

Figure 15: Variation of bulk temperature with channel height for various values of ω. (a) K is constant, $\tau = 0.25$; and (b) K is variable, $0.125 \leq \tau \leq 0.5$.

3. Occurrence of flow reversal is delayed to higher values of Gr/Re, with an increase of ε in the range of $0 \leq \varepsilon \leq 1$, and this is more distinct when ε varies from 0 to 0.5.
4. Except $\omega = 1$, denoting the no radiation condition, as scattering albedo varies between 0 and 0.75, radiation effects on the flow and thermal fields for the constant and variable extinction coefficient are entirely opposite.
5. For constant K, as ω decreases from 0.75 to 0, fluid flow reaches its hydrodynamically and thermally developed state more rapidly. Also, the bulk temperature increases more quickly and reaches the wall temperature. Moreover, fRe is reduced by a decrease in ω, due to the reduction of the buoyancy force effect. For variable K, all these are entirely opposite.
6. The radiative wall heat flux is not considerably affected by the variation of ω when K is constant. However, for variable K, as ω decreases, it increases slightly. Also, at the entrance region of the channel, the total heat flux is greater than that for constant K, especially for lower values of ω.
7. Except $\omega = 1$, the occurrence of flow reversal is postponed to higher values of Gr/Re, with an increase of ω, while K is variable. But for the constant K condition, the threshold value of Gr/Re falls with a rise in ω.

References

[1] Bejan, A., *Convection Heat Transfer*, second ed., John Wiley and Sons, USA (1995).

[2] Brinkworth, B.J. "A procedure for the routine calculation of laminar free and mixed convection in inclined ducts", *Int. J. Heat Fluid Flow*, 21, pp. 456–462 (2000).

[3] Gau, C., Jeng, Y.C. and Liu, C.G. "An experimental study on mixed convection in a horizontal rectangular channel heated from a side", *J. Heat Transfer*, 122, pp. 701–707 (2000).

[4] Behzadmehr, A., Galanis, N. and Laneville, A. "Flow reversal in laminar mixed convection", *ASME Int. Mech. Engrg. Congress and Exposition*, New York, USA, HTD-Vol. pp. 369–1 (2001).

[5] Boulama, K. and Galanis, N. "Analytical solution for fully developed mixed convection between parallel vertical plates with heat and mass transfer", *J. Heat Transfer*, 126, pp. 381–388 (2004).

[6] Dogan, A., Sivrioglue, M. and Baskaya, S. "Experimental investigation of mixed convection heat transfer in a rectangular channel with discrete heat sources at the top and at the bottom", *Int. Commun. Heat Mass Transfer*, 32, pp. 1244–1252 (2005).

[7] Fiveland, W.A. "Discrete ordinates solutions of the radiative transport equation for rectangular enclosures", *ASME J. Heat Transfer*, 106, pp. 699–706 (1984).

[8] Fiveland, W.A. "Three dimensional radiative heat transfer solutions by discrete ordinates method", *J. Thermophys. Heat Transfer*, 2(4), pp. 309–316 (1988).

[9] Kim, T.Y. and Baek, S.W. "Analysis of combined conductive and radiative heat transfer in a two-dimensional rectangular enclosure using the discrete ordinates method", *Int. J. Heat Mass Transfer*, 34(9), pp. 2265–2273 (1991).

[10] Baek, S.W. and Lee, H.J. "An unsteady conduction and two-phase radiation in a 2-D rectangular enclosure with gas and particles", *Numer. Heat Transfer Part A: Appl.*, 41(3), pp. 285–305 (2002).

[11] Yang, G. and Ebadian, M.A. "Thermal radiation and laminar forced convection in the entrance region of a pipe with axial conduction and radiation", *Int. J. Heat Fluid Flow*, 12(3), pp. 202–209 (1991).

[12] Yan, W.M. and Li, H.Y. "Radiation effects on mixed convection heat transfer in a vertical square duct", *Int. J. Heat Mass Transfer*, 44, pp. 1401–1410 (2001).

[13] Krishnan, A.S., Premachandran, B., Balaji, C. and Venkateshan, S.P. "Combined experimental and numerical approaches to multi-mode heat transfer between vertical parallel plates", *Exp. Thermal Fluid Sci.*, 29, pp. 75–86 (2004).

[14] Yan, W.M. and Li, H.Y. "Radiation effects on laminar mixed convection in an inclined square duct", *ASME J. Heat Transfer*, 121, pp. 194–200 (1999).

[15] Talukdar, P. and Simonson, C.J. "Effect of axial radiation on heat transfer in a thermally and hydrodynamically developing flow between parallel plates", *Numer. Heat Transfer Part A*, 52(10), pp. 911–934 (2007).

[16] Rao, C.G. "Interaction of surface radiation with conduction and convection from a vertical channel with multiple discrete heat sources in the left wall", *Numer. Heat Transfer Part A*, 52(9), pp. 831–848 (2007).

[17] Bazdidi-Tehrani, F. and Nezamabadi, M. "Effect of Gr/Re on mixed convection and combined mixed convection–radiation heat transfer within a vertical channel with variable wall temperature", *Sci. Iranica*, 12(3), pp. 178–189 (2005).

[18] Cheng, C.H., Weng, C.J. and Aung, W. "Buoyancy-assisted flow reversal and convective heat transfer in entrance region of a vertical rectangular duct", *Int. J. Heat Fluid Flow*, 21, pp. 403–411 (2000).

[19] Chamkha, A.J. "On laminar hydromagnetic mixed convection flow in a vertical channel with symmetric and asymmetric wall heating condition", *Int. J. Heat Mass Transfer*, 45, pp. 2509–2525 (2002).

[20] Jeng, Y.N., Chen, J.L. and Aung, W. "On the Reynolds-number independence of mixed convection in a vertical channel subjected to asymmetric wall temperatures with and without flow reversal", *Int. J. Heat Fluid Flow*, 13(4), pp. 329–339 (1992).

[21] Barletta, A. "Analysis of flow reversal for laminar mixed convection in a vertical rectangular duct with one or more isothermal walls", *Int. J. Heat Mass Transfer*, 44, pp. 3481–3497 (2001).

[22] Barletta, A. "Fully developed mixed convection and flow reversal in a vertical rectangular duct with uniform wall heat flux", *Int. J. Heat Mass Transfer*, 45, pp. 641–654 (2002).

[23] Ingham, D.B., Keen, J. and Heggs, P.J. "Two dimensional combined convection in vertical parallel plate ducts including situations of flow reversal", *Int. J. Numer. Methods Eng.*, 26, pp. 1645–1664 (1988).

[24] Desrayaud, G. and Lauriat, G. "Flow reversal of laminar mixed convection in the entry region of symmetrically heated, vertical plate channels", *Int. J. Thermal Sciences*, 48, pp. 2036–2045 (2009).

[25] Bazdidi-Tehrani, F. and Shahini, M. "Combined mixed convection–radiation heat transfer within a vertical channel: investigation of flow reversal", *J. Numer. Heat Transfer, Part A*, 55(3), pp. 289–307 (2009).

[26] Wang, M., Tsuji, T. and Nagano, Y. "Mixed convection with flow reversal in the thermal entrance region of horizontal and vertical pipe", *Int. J. Heat Mass Transfer*, 37, pp. 2305–2319 (1994).

[27] Siegel, R. and Howell, J.R., *Thermal Radiation Heat Transfer*, third ed., McGraw-Hill Book Company, New York, USA (1992).
[28] Patankar, S.V., *Numerical Heat Transfer and Fluid Flow*, McGraw-Hill, UK (1980).

Farzad Bazdidi-Tehrani completed his M.S. and Ph.D. degrees at Leeds University, UK. He joined the School of Mechanical Engineering at Iran University of Science and Technology (IUST) in 1991 and, since then has been active in both teaching and research. Dr. Tehrani has taught several courses at both undergraduate and graduate levels, namely, Heat Transfer, Convection, Thermal Radiation, Boundary Layers Theory etc. His current research fields of interest include: Modeling of Cooling Techniques Related to Hot Sections in Gas Turbine Engines and Electronic Components, Combined Heat Transfer (Mixed Convection–Radiation) in Channels, Two-Phase Flow (Boiling) and Turbulent Reactive Flows.

Hadi Nazaripoor obtained his B.S. degree from Guilan University, with merit. He has recently completed his M.S. degree in Energy Conversion at the Department of Mechanical Engineering, Iran University of Science and Technology, with distinction. He is now planning to pursue his studies at the Ph.D. degree level. His current research field is focused on the CFD Modeling of Various Heat Transfer Phenomena in Vertical and Inclined Channels.